Available online at www.sciencedirect.com

ScienceDirect

Materials Today: Proceedings 3 (2016) 3094–3103

www.materialstoday.com/proceedings

ARRMA-2016

Effect of Alloying Additions and Heat Treatment on the Microstructure Evolution of Nb─16Si Alloy

M.Sankar[a,b]*, G.Phanikumar[b], V.V.Satya Prasad[a]

[a]*Defence Metallurgical Research Laboratory, Kanchanbagh, Hyderabad-500058, India*
[b]*Department of Metallurgical and Materials EngineeringInstitute, Indian Institute of Technology Madras, Chennai-600036, India*

Abstract

In this study, the effect of Ta, Ni, Zr additions and heat treatment on the microstructure and hardness of Nb–16Si have been investigated. It was observed that Ta addition has not changed the microstructure of the alloy, while Ni and Zr additions drastically changed the microstructure of the alloys. The alloying additions increased the hardness of the alloys in as cast condition. However, hardness of phases present in the alloy decreased after heat treatment. Nb_{ss} and Nb_3Si phases were observed in Nb–16Si and Nb–16Si–3Ta alloys while Nb_{ss} and Nb_5Si_3 phases were observed in Nb–16Si–3Ni and Nb–16Si–3Zr alloys after heat treatment.

Selection and Peer-review under responsibility of Conference Committee Members of Advances in Refractory and Reactive Metals and Alloys (ARRMA-2016).

Keywords: Niobium silicide; gas turbine, eutectoid transformation, heat treatment.

---

* Corresponding author. Tel.:+91-040-24586770; fax: +91-040-24342316.
E-mail address: msankar.iitk@gmail.com

Selection and Peer-review under responsibility of Conference Committee Members of Advances in Refractory and Reactive Metals and Alloys (ARRMA-2016).

1. Introduction

Alloys based on the Nb–Si system have been considered as a potential candidate for the next generation gas turbine blade material with significantly higher operating temperatures than the currently used Ni-based superalloys, because of their high melting point (>1750 ºC), relatively low density (6.6 – 7.2 kg/cc), excellent high temperature strength and very good creep resistance [1–3]. However, poor oxidation resistance and room temperature fracture toughness limits these alloy use for high temperature applications. The potential applications of these alloys at very high temperature require a balance of high creep strength, good oxidation resistance and acceptable low-temperature fracture toughness.

Nb–Si system forms in situ composites where niobium solid solution (Nb_{ss}) phase is dispersed in continuous matrix of silicides, which includes Nb_5Si_3, Nb_3Si or both depending upon the Si content [4, 5]. The niobium solid solution phase provides room temperature fracture toughness and silicide phase (Nb_5Si_3) provides high temperature strength and creep resistance. In the binary Nb–Si alloy, the metastable Nb_3Si phase is retained at room temperature due to the sluggish nature of decomposition of Nb_3Si phase in to Nb_5Si_3 phase during solidification [6, 7]. Moreover, Nb–Si alloy with Nb_3Si phase has poor creep properties [8–10**].** Long duration (>100 hrs) heat treatment at 1500° C and above is required to convert Nb_3Si phase in to stable equilibrium Nb_{ss} + Nb_5Si_3 phases through eutectoid reaction [10, 11]. These Nb and Nb_5Si_3 phases are thermodynamically stable and impart adequate creep strength at elevated temperatures.

Alloying additions play an important role in controlling the microstructure of Nb–Si alloy and tailoring the optimum combination of properties. Earlier studies have shown that elements such as Ti, Hf, Zr, Cr, Al, Mo, W, Fe and Sn have been added to Nb–Si alloys with Si concentrations in the range 12–22 at% [12–17]. Among the alloying elements studied it has been reported that addition of Ti and Hf to Nb–Si alloys have shown positive effect on improving room temperature fracture toughness and oxidation resistance [18–20]. However, higher Ti and Hf concentrations can have adverse effects on creep performance [21, 22]. The addition of Mo and W can enhance high temperature strength by solid solution strengthening [23–24]. The additions of Al, Cr and Sn can improve the oxidation resistance [12, 14]. Small quantity of Zr addition has been reported to accelerate eutectoid decomposition reaction of Nb_3Si phase [16, 17]. To date, the reports on the effect of Ta, Ni and Zr additions on the microstructure and mechanical properties of Nb–Si alloys are still poor. Hence, in the present work, the effect of Ta, Ni, Zr additions on the microstructure and mechanical properties of Nb–16Si has been investigated.

2. Experimental

The nominal compositions of the alloys investigated in this work are Nb–16Si, Nb–16Si–3Ta, Nb–16Si–3Ni and Nb–16Si–3Zr. The compositions are reported in atomic percent unless otherwise stated. High purity Nb (99.9), Si (99.999), Ta (99.9), Ni (99.9) and Zr (99.9) were used as starting materials. The alloys were prepared by non - consumable arc melting method using a tungsten electrode under an argon atmosphere in water cooled copper crucible. Each alloy was remelted five times to ensure chemical homogeneities. The alloys were cut by electro discharge machining (EDM) wire cut for heat treatment and microstructural observations. Heat treatment was carried out in an alumina tubular furnace at 1400 ºC in vacuum for 50 and 100 h and then furnace cooled. Samples for microstructures were mounted in Bakelite and mechanically polished to 0.5 µm finish. Microstructures of the as cast and heat treated alloys were observed using JSM 5800® scanning electron microscope (SEM) equipped with energy dispersive X-ray spectroscopy (EDS). The chemical compositions of different phases present in the alloys were determined with help of energy dispersive X-ray spectroscopy (EDS) and CAMECA® electron probe micro analyser (EPMA). X-ray diffraction was performed using Philip 3710® diffractometer on bulk samples to identify the phase constituents using Cu k_{α} (λ=0.15405 nm) radiation at 40 kV. JCPDC data were used for identification of the different phases. Volume fraction of different phases exist in the alloys were measured by image analyser using images obtained from back scattered SEM. Microhardness of each phase of the alloys was measured on metallography samples using Leica® VMHT auto Vickers microhardness testing machine with load of 10 gf and holding time of 15 seconds. A minimum of 10 indentations were taken for microhardness of selected phases.

3. Results and Discussion

The XRD patterns of as cast Nb–16Si, Nb–16Si–3Ta, Nb–16Si–3Ni and Nb–16Si–3Zr alloys are shown in Fig. 1. Niobium solid solution (Nb_{ss}) and Nb_3Si peaks are observed in Nb–16Si and Nb–16Si–3Ta, while, in the case of Nb–16Si–3Ni and Nb–16Si–3Zr alloys, Nb_5Si_3 peaks are observed along with Nb_{ss} and Nb_3Si peaks. The typical SEM backscattered electron images of alloys are shown in Fig. 2. It was observed that Nb–16Si and Nb–16Si–3Ta alloys reveal the presence of a two phase microstructures consisting of Nb_{ss} and Nb_3Si phases, whereas Nb–16Si–3Ni and Nb–16Si–3Zr alloys reveal the presence of three phase microstructures consisting of Nb_{ss}, Nb_3Si and Nb_5Si_3 phases. The overall chemical composition of the alloys and chemical compositions of different phases present in the alloys are shown in Table 1. It has been depicted from the microstructure (Fig. 2. a) that the addition of Ta does not show significant influence on the microstructure and morphology of phases. The addition of Ni has resulted in significant changes in the microstructure and the morphology of Nb_{ss} and Nb_3Si phases besides formation of Nb_5Si_3 phase (Fig. 2. c). The Nb–16Si–3Ni alloy also reveals very fine eutectic mixture of Nb_{ss} and Nb_3Si phases. Similar to Ni addition, the addition of Zr also resulted in a drastic change in the microstructure and morphology of phases (Fig. 2. d). The eutectic mixture is completely lamellar along with the coarse dendrites of primary Nb_{ss} phase. It is known from Fig. 1 and Fig. 2 that the addition of Ni and Zr resulted in promotion of Nb_5Si_3 phase during solidification.

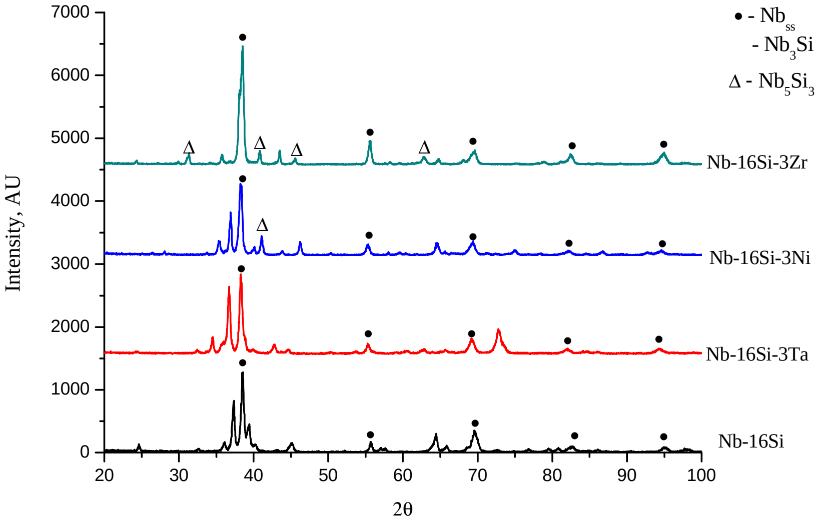

Fig. 1. XRD Pattern of alloys in as cast condition.

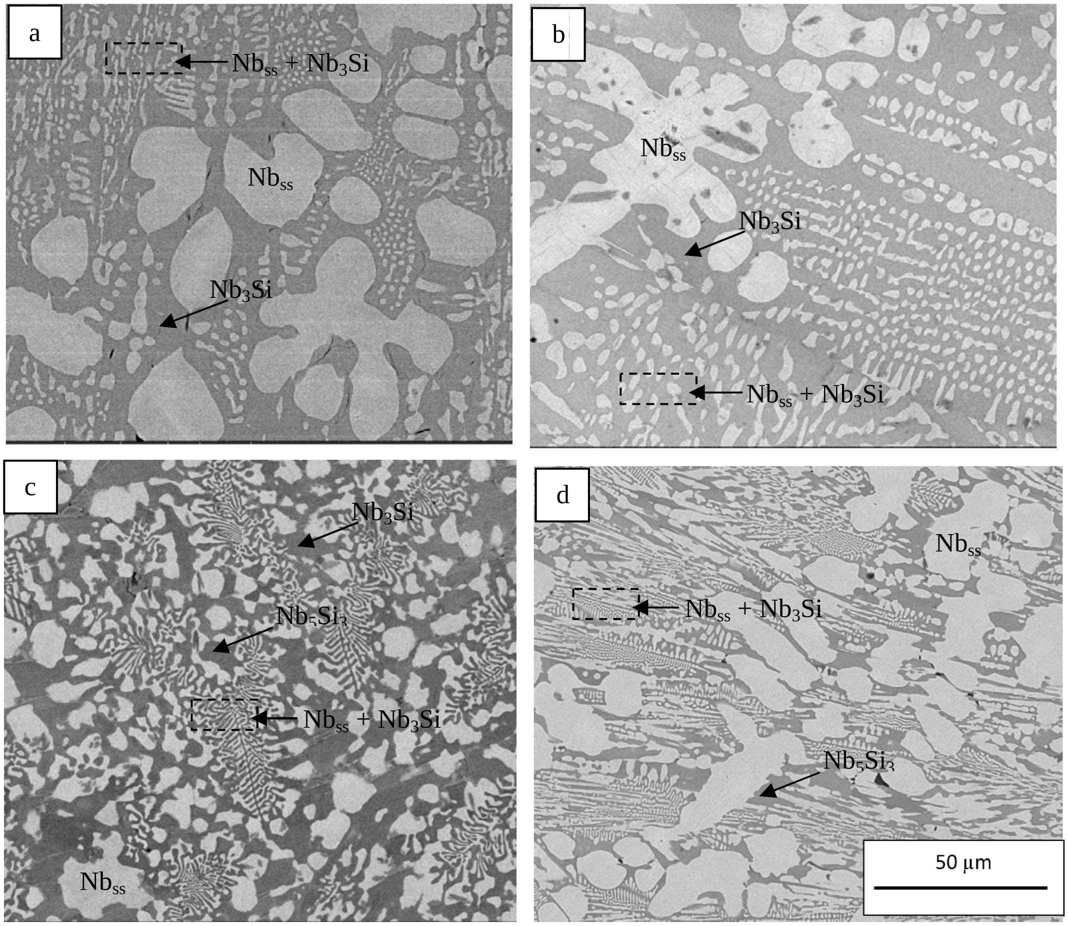

Fig. 2. SEM micrograph of alloys in as cast condition: (a) Nb–16Si, (b) Nb–16Si–3Ta, (c) Nb–16Si–3Ta and (d) Nb–16Si–3Zr.

Table 1. The phases present in the alloys and their compositions (at. %) determined by EDS.

Alloy composition	Phases	Nb	Si	Ta	Ni	Zr
Nb–16Si	Overall	81.9	16.1	-	-	-
	Nb_{ss}	94.6	5.4	-	-	-
	Nb_3Si	77.2	22.8	-	-	-
Nb–16Si–3Ta	Overall	81.9	15.00	3.1	-	-
	Nb_{ss}	92.8	3.6	3.6	-	-
	Nb_3Si	74.2	21.7	3.1	-	-
Nb–16Si–3Ni	Overall	80.9	16.1	-	3.0	-
	Nb_{ss}	95.8	3.1	-	1.1	-
	Nb_3Si	72.2	21.4	-	6.4	-
	Nb_5Si_3	67.0	28.0	-	5.0	-
Nb–16Si–3Zr	Overall	80.8	16.4	-	-	2.8
	Nb_{ss}	96.2	3.2	-	-	0.6
	Nb_3Si	70.7	24.3	-	-	5.0

The volume fractions of the alloys studied are shown in Table 2. It has been observed that the volume fractions of Nb$_{ss}$ and Nb$_3$Si phases in the Nb–16Si alloy are approximately 55.4 % and 44.6% respectively. The volume fractions of Nb$_{ss}$ and Nb$_3$Si phases in Nb–16Si–3Ta alloy are 63.3% and 36.7% respectively. Here the volume fraction of Nb$_{ss}$ phase is more as compared to Nb–16Si alloy. This may be due to the partition of Ta is more in Nb$_{ss}$ phase than in Nb$_3$Si phase. For Nb–16Si alloy containing Ni, the volume fraction of Nb$_{ss}$ phase is 51.7% and Nb$_3$Si and Nb$_5$Si$_3$ phases are 25.3 % and 23.0 % respectively, while Nb–16Si alloys containing Zr, the volume fraction of Nb$_{ss}$ phase is 63.6% and Nb$_3$Si phase is 36.4%.

Table 2. Volume fraction of alloys measured in as cast condition.

Alloy composition	Volume fraction (%)		
	Nb$_{ss}$	Nb$_3$ Si	Nb$_5$ Si
Nb–16Si	55.4	44. 6	-
Nb–16Si–3Ta	63.3	36.7	-
Nb–16Si–3Ni	51.7	25.3	23.0
Nb–16Si–3Zr	63.6	36.4	-

The XRD patterns of alloys heat treated at 1400 ºC for 50 h are shown in Fig. 3. The Nb–16Si and Nb–16Si–3Ta alloys show presence of Nb$_{ss}$ and Nb$_3$Si peaks, while Nb–16Si–3Ni and Nb–16Si–3Zr alloys show presence of Nb$_{ss}$ and Nb$_5$Si$_3$ peaks. SEM backscattered electron images of alloys heat treated at 1400 ºC for 50 h are shown in Fig. 4. There were no significant changes in microstructure and morphology observed in Nb–16Si alloy while significant changes in microstructure and morphology observed in Nb–16Si–3Ta, Nb–16Si–3Ni and Nb–16Si–3Zr alloys. It is observed from XRD pattern and microstructure (Fig. 3 and Fig. 4) that minor fraction of Nb$_5$Si$_3$ phase is seen observed in Nb-16Si alloy. It indicates that the eutectoid transformation reaction has been initiated during heat treatment. The chemical compositions of the phases present in the alloys after heat treatment at 1400 ºC for 50h is shown in Table 3.

Table 3. Compositions of the phases present in the alloys determined by EPMA after heat treatment at 1400 ºC for 50 h.

Alloy composition	Phases	Nb	Si	Ta	Ni	Zr
Nb–16Si	Nb$_{ss}$	96.8±0.16	3.2±0.16	-	-	-
	Nb$_3$Si	75.3±0.09	24.7±0.09	-	-	-
Nb–16Si–3Ta	Nb$_{ss}$	94.2±0.11	1.7±0.09	4.1±0.08	-	-
	Nb$_3$Si	70.9±0.63	24.6±0.28	4.5±0.36	-	
Nb–16Si–3Ni	Nb$_{ss}$	97.6±0.24	1.9±0.18	-	0.5±0.06	-
	Nb$_5$Si$_3$	66.8±0.07	28.0±0.22	-	5.2±0.17	-
Nb–16Si–3Zr	Nb$_{ss}$	97.0±0.2	2.4±0.16	-	-	0.6±0.05
	Nb$_3$Si	73.6±0.11	25.2±0.1	-	-	1.3±0.04
	Nb$_5$Si$_3$	58.5±0.2	36.5±0.25	-		5.0±0.05

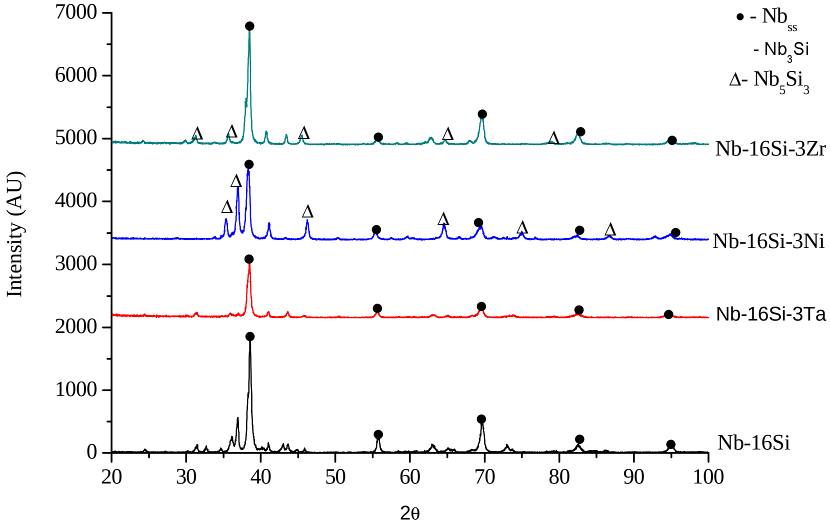

Fig. 3. XRD Pattern of alloys heat treated at 1400 °C for 50h.

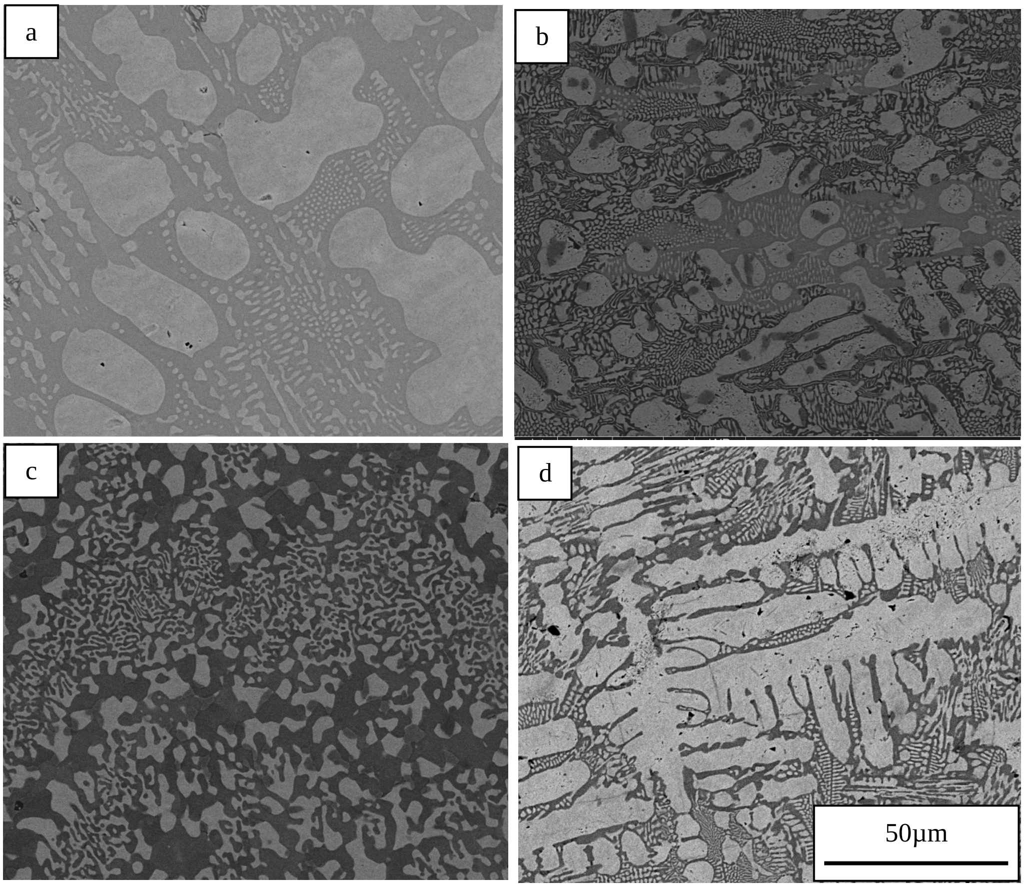

Fig. 4. SEM micrograph of alloy heat treated for 50 h: (a) Nb–16Si, (b) Nb–16Si–3Ta, (c) Nb–16Si–3Ni and (d) Nb–16Si–3Zr.

Fig. 5. Shows the XRD patterns of alloys heat treated at 1400 ºC for 100h. It was noted that all the Nb_{ss}, Nb_3Si and Nb_5Si_3 peaks were seen in Nb–16Si and Nb–16Si–3Ta alloys. However, several peaks from the untransformed Nb_3Si phase are present in these samples. It indicates that eutectoid transformation has not been completed in Nb–16Si and Nb–16Si–3Ta alloys. The Nb–16Si–3Ni and Nb–16Si–3Zr alloys have shown only Nb_{ss} and Nb_5Si_3 peaks which shows significant evidence of completion of eutectoid transformation of Nb_3Si. The microstructures of alloys heat treated at 1400 ºC for 100 h are shown in Fig. 6. A significant change in microstructure and morphology of different phases present in all the alloys. The phases observed in Nb–16Si and Nb–16Si–3Ta alloys are Nb_{ss} and Nb_3Si along with Nb_5Si_3. In contrary in Nb–16Si–3Ni and Nb–16Si–3Zr alloys only Nb_{ss} and Nb_5Si_3 phases are observed. It has been observed from Fig. 5 and Fig. 6 eutectoid transformation of Nb_3Si phase has not been completed Nb–16Si and Nb–16Si–3Ta alloys during heat treatment, whereas complete eutectoid transformation of Nb_3Si phase has been taken place in The Nb–16Si–3Ni and Nb–16Si–3Zr alloys. The microstructure of the eutectic mixture has become refined in all the four alloys after heat treatment. Moreover, it is also noted that Ni and Zr additions to Nb-Si alloy accelerate eutectoid transformation (Nb_3Si to Nb_5Si_3 + Nb_{ss}) reaction. The XRD results of alloy heat treated at 1400 ºC for 100 h (Fig. 5) also confirms the presence of Nb_5Si_3 phase in Nb–16Si–3Ni and Nb–16Si–3Zr alloys.

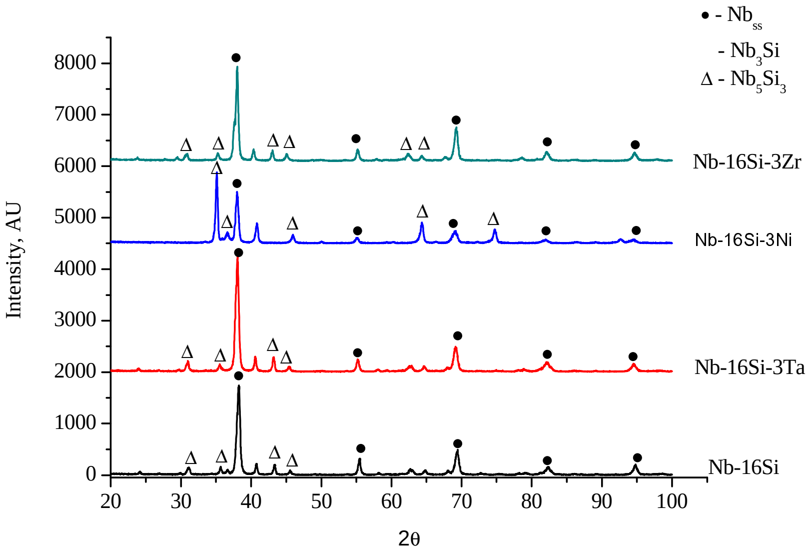

Fig. 5. XRD Pattern of alloys heat treated at 1400 ºC for 100h

Table 4. Hardness of the alloys in as cast and heat treated conditions.

Alloy composition	Vickers Microhardness (Hv), Load : 10gf							
	As cast				Heat treated at 1400 ºC for 50h			
	Nb_{ss}	Nb_3 Si	Nb_5Si_3	Eutectic mixture	Nb_{ss}	Nb_3 Si	Nb_5Si_3	Eutectic mixture
Nb–16Si	454±11.6	924±14.7	-	921±15.3	280±17.5	1070±20.4	-	726±18.9
Nb–16Si–3Ta	542±12.5	1230±20	-	1015±21.3	358±7.4	1222±20.5	-	757±19.7
Nb–16Si–3Ni	582±15.8	1578±22.5	1600±25	867±22	513±19.3	1310±28.5	1550±19.2	806±10.5
Nb–16Si–3Zr	598± 9.8	1218± 14.9	-	804±18	289±7.5	1100 ±15.3	1300±14.9	880±15.2

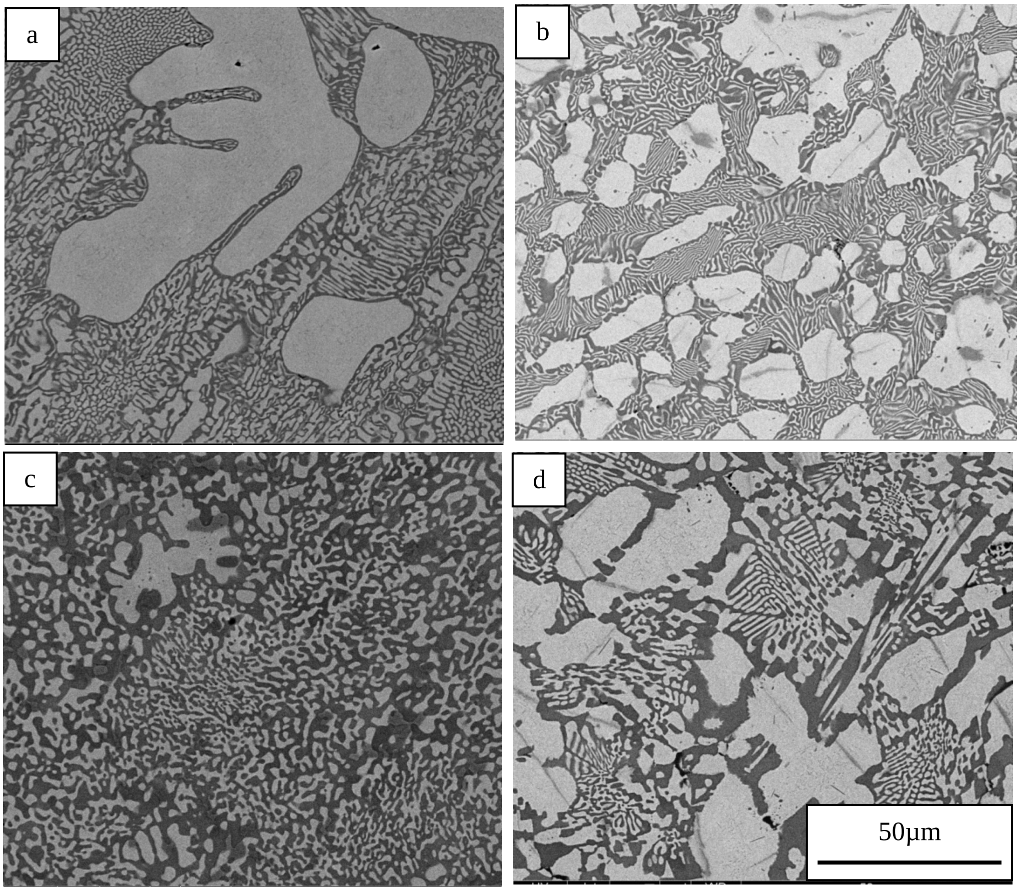

Fig. 6. SEM micrograph of alloy heat treated for 100 h: (a) Nb−16Si, (b) Nb−16Si−3Ta, (c) Nb−16Si−3Ni and (d) Nb−16Si−3Zr.

Table 5. Compositions of the phases present in the alloys determined by EPMA after heat treatment at 1400 °C for 100 h.

Alloy composition	Phases	Nb	Si	Ta	Ni	Zr
Nb−16Si	Nb_{ss}	96.4±0.35	3.6±0.35			
	Nb_3Si	75.5±0.45	24.5±0.45			
	Nb_5Si_3	65.1±0.5	34.9±0.5			
Nb−16Si−3Ta	Nb_{ss}	92.2±0.13	3.0±0.09	4.8±0.21		
	Nb_3Si	72.1±0.55	25.4±0.55	2.5±0.1		
	Nb_5Si_3	62.8±0.37	34.6±0.31	2.6±0.05		
Nb−16Si−3Ni	Nb_{ss}	94.7±0.29	5.0±0.25	-	0.3±0.04	-
	Nb_5Si_3	66.6±0.15	28.3±0.19	-	5.1±0.05	-
Nb−16Si−3Zr	Nb_{ss}	97.0±0.2	2.2±0.17	-	-	0.8±0.2
	Nb_5Si_3	58.2±0.14	36.7±0.11	-	-	5.3±0.07

The hardness of alloys in as cast and heat treated conditions is listed in Table 4. The hardness of Nb_{ss} and eutectic mixture in as cast condition is higher than as in heat treated condition. The decrease in hardness after heat treatment is due to the precipitation of Nb_5Si_3 phase in Nb_{ss} during heat treatment. This precipitation of Nb_5Si_3 phase in Nb_{ss} resulted in lowering the solid solution strengthening of Nb_{ss} phase. However, the decrease in hardness is very marginal in Nb−16Si−3Ni alloy. The compositions of the phases present in the alloys heat treated at 1400 ºC for 100 h is shown in Table 5. It is observed from Table 3 and Table 5 that the Ta is predominantly portioned in Nb phase, while Ni and Zr portioned in Nb_5Si_3 phase.

4. Conclusions

1. Ta addition has two phase microstructures consisting of Nb_{ss} and Nb_3Si phases whereas Ni and Zr addition have three phase microstructures consisting of Nb_{ss}, Nb_3Si and Nb_5Si_3 phases in as cast condition.
2. Ta addition does not have any significant role on the microstructure, while Ni and Zr additions have shown significant influence on the microstructure changes.
3. A complete eutectoid transformation of Nb_3Si phase has been taken in Nb−Si alloy containing Ni and Zr. A partial eutectoid transformation of Nb_3Si phase has been observed in Nb−Si and Nb−Si−Ta alloys.
4. Additions of Ta, Ni, and Zr increase the hardness of both Nb_{ss} and Nb_3Si phases. The hardness of eutectic mixture increases with Ta addition and decreases with Ni and Zr additions.

Acknowledgement

The authors are grateful to Defence Research and Development Organisation, Ministry of Defence, New Delhi for the financial support in carrying out this research work. The authors wish to thank Dr. S. V. Kamat, Director, DMRL for his keen interest and encouragement. The authors also would like to thank officers and staff of electroslag remelting group and electron microscopy group for giving technical support to carry out this work

References

[1] Bewley BP, Jackson MR, Zhao J C, Subramanian PR, Mendiratta MG, Lewandowski JJ. Ultrahigh−temperature Nb−Silicide based composites. MRS Bull. 2003; 646–653.

[2] Bewley BP, Lipsitt HA, Jackson MR, Reeder WJ, Sutliff JA. Solidification processing of high temperature intermetallic eutectic−based alloy. Mater. Sci. Eng A., 1995; 192–193: 534 –543.

[3] Bewley BP, Jackson MR, Zhao Z C, Subramanian P R. A review of very high temperature Nb-silicide based composites. Metall. Mater. Trans. A 2003; 34: 2043–2052.

[4] Zhao J C, Westbrook JH. Ultrahigh- temperature materials for jet engines .MRS Bull.2003; 28 (9): 622–630.

[5] Miura S, Murasato Y, Sekido Y, Tsutsumib Y, Ohkuboa K, Kimurac Y, Mishimac Y, Mohria T. Effect of microstructure on the high-temperature deformation behaviour of Nb–Si alloys. Mater. Sci. Eng A., 2009; 510–511: 317–321.

[6] Sekido N, Kimura Y, Miura S, Wei FG, Mishima Y. Fracture toughness and high temperature strength of unidirectionally solidified Nb−Si binary and Nb−Ti−Si ternary alloys. J. Alloys compd. 2006; 425: 223–229.

[7] Subramanian PR, Mendiratta MG, Dimiduk DM. Microstructures and mechanical behavior of Nb-Ti base beta + silicide alloy. Mater. Res .Soc. Symp. Proc. 1994; 322: 491.

[8] Chan K S. Modelling creep behaviour of niobium silicide in-situ composites. Mater. Sci. Eng A., 2002; 337: 59 – 66.

[9] Bewley BP, Sitzman SD, Brewer LN, Jackson MR. Analyses of eutectoid phase transformations in Nb – Silicide in situ composites. Microsc. Microanal 2004; 10: 470−480.

[10] Mendiratta MG, Dimiduk DM. Phase relations and transformation kinetics in the high Nb region of the Nb−Si system. Scripta Metall. 1991; 25(1): 237–242.

[11] Miura S, Kim JH, Ohkubo K, Kimura Y, Sekido N, Mishima Y, Morhi T. Microstructural control of Nb−Si alloy with invariant reactions. Mater. Sci. Forum. 2007; 539–543: 1507–1512.

[12] Vellios N, Tsakiropoulos P. The role of Sn and Ti additions in the microstructure of Nb–18Si base alloys. Intermetallics. 2007; 15 (12): 1518–1528.

[13] Grammenos I, Tsakiropoulos P. Study of the role of Mo and Ta additions in the microstructure of Nb–18Si–5Hf silicide based alloy. Intermetallics. 2010; 18 (8): 1524–1530.

[14] Vellios N, Tsakiropoulos P. Study of the role of Al, Cr and Ti additions in the microstructure of Nb–18Si–5Hf alloys. Intermetallics. 2010; 18 (2):242–253.

[15] Tian YX, Guo JT, Sheng L Y, Cheng GM, Zhou LZ, He L L, Ye H Q. Microstructure and mechanical properties of cast Nb–Ti–Si–Zr alloys. Intermetallics. 2008; 16: 807–812.

[16] Miura S, Aoki M, Saeki Y, Ohkubo K, Mishima Y, Mohri T. Effects of Zr on the eutectoid decomposition of behaviour of Nb_3Si in to (Nb)/Nb_5Si_3. Metall. Mater. Trans. A. 2005; 36(30): 489–496.

[17] Miura S, Ohkubo K, Mohri T. Microstructural control of Nb–Si alloy for large Nb grain formation through eutectic and eutectoid reactions. Intermetallics. 2007; 15:783–790.

[18] Chan KS, Davidson DL. Effects of Ti addition on cleavage fracture in Nb–Cr–Ti solid solution alloys. Metall. Materi. Trans. A. 1999; 30(4): 925–939.

[19] Chan KS, Davidson DL. Improving the fracture toughness of constituent phases and Nb–based in–situ composites by a computational alloy design approach. Metall. Mater.Trans A. 2003; 34:1833–1849.

[20] Tian YX, Guo JT, Zhou LT, Cheng GM, Ye HQ. Microstructure and room temperature toughness of cast Nbss/Silicides composites with Hf. Mater. Lett. 2008; 62(16–17): 2657–2660.

[21] Bewlay BP, Briant CL, Davis AW, Jackson MR. The effect of silicide volume fraction on the creep behaviour of Nb-silicide based in-situ composites. Mater. Res. Soc Symp. Proc. 2000; 646.

[22] Bewlay BP, Grylls RJ, Fraser HL. On the formation of silicide precipitates in niobium–silicide based composites. Mater. Res .Soc. Symp. Proc. 1998; 552.

[23] Kim WY, Tanaka H, Kasam A, Hanada S. Microstructure and room temperature fracture toughness of Nb_{ss} and Nb_5Si_3 composites. Intermetallics. 2001; 9(9): 827–834

[24] Kim WY, Tanaka H, Kasam A, Hanada S. Microstructure and high temperature strength at 1773K of Nbss/Nb_5Si_3 composites alloyed with molybdenum. Intermetallics. 2002; 10 (6): 625–634